



Multi-plane augmented reality display based on cholesteric liquid crystal reflective films

QUANMING CHEN,¹ ZENGHUI PENG,² YAN LI,^{1,*} SHUXIN LIU,¹ PENGCHENG ZHOU,¹ JINGYUAN GU,¹ JIANGANG LU,¹ LISHUANG YAO,² MIN WANG,³ AND YIKAI SU¹

¹Department of Electronic Engineering, Shanghai Jiao Tong University, Shanghai, 200240, China

²Changchun Institute of Optics, Fine Mechanics and Physics, Chinese Academy of Sciences, Changchun, 130033, China

³Department of General Surgery, Shanghai General Hospital, Shanghai Jiao Tong University, Shanghai, 200025, China

*yan.li@sjtu.edu.cn

Abstract: To address the accommodation-convergence conflict problem in conventional augmented reality (AR) head-mounted displays, we propose a compact multi-plane display design based on cholesteric liquid crystal (CLC) reflective films and a polarization switch. Because of the polarization selectivity of CLC films, circularly-polarized light with different handedness is reflected by different CLC films, resulting in different optical path lengths and different image depths by the lens. A flicker-free dual-plane prototype with correct focus cues and relatively low operating voltage has been implemented. Moreover, a multi-plane AR display scheme with more than 2 depth planes is proposed by stacking multiple CLC films and polarization switches together.

© 2019 Optical Society of America under the terms of the [OSA Open Access Publishing Agreement](#)

1. Introduction

Augmented reality (AR) technology, which enables users to see digitally generated virtual information augmented on real surroundings, offers new experience in various fields, such as education, entertainment, etc. However, most AR headsets, such as Microsoft HoloLens and Meta, employ the binocular stereoscopic display technique [1] to generate virtual 3D images. The intrinsic depth cues mismatch between accommodation and convergence originating from this display technique causes eye fatigue and discomfort for users [2]. To overcome this problem, researchers have employed true 3D display techniques, such as holographic display [3,4], integral imaging display [5,6], super multi-view display [7,8], and volumetric display [9,10].

Multi-plane display [9–17] is the most commonly used volumetric display technique for AR applications. It generates 3D images by cutting a 3D scene into 2D image slices, and displaying them in different depths. Liu et al. and Lee et al. proposed, multi-plane displays for AR applications based on sequential switching of scattering films, using polymer-stabilized liquid crystal (PSLC) [11,12] and polymer-stabilized cholesteric liquid crystal (PSCLC) [13], respectively. However, both PSLC and PSCLC films, require relatively high switching voltage. Recently, a few works have been reported on multi-plane AR displays based on polarization multiplexing, where the requirement for operating voltage is loosened [14–16]. Love et al. proposed a multi-focus display employing ferroelectric liquid-crystal polarization switches and birefringent lenses [14]. Wu et al. presented a near-eye multi-plane display using a fast-response switchable lens based on a twisted-nematic (TN) liquid crystal polarization switch [15]. And Lee et al. designed a compact multi-focus display with a Savart plate [16]. Nevertheless, it is difficult to realize more than two image planes while maintaining a compact form factor.

In this paper, we propose a compact multi-plane AR display design based on reflective CLC films [17–19]. Thanks to the polarization selective reflectivity of CLC films, circularly-polarized light with different handedness is reflected by different CLC films, generating images at different depths in time sequence, with the aid of a fast-response polarization switch. A monochrome dual-plane display prototype was implemented at video rate. The feasibility of realizing color display with CLC films was experimentally verified. In the end, a multi-plane display design with more than 2 planes was proposed and experimentally verified. With correct depth cues and compact form factor, we believe our display design has great potential in augmented reality 3D displays.

2. Principle

Figure 1(a) shows the design of the multi-plane AR display system using two CLC films. It mainly consists of five parts: an image source, a polarization switch, a beam splitter (BS), a lens and two CLC films. The polarization switch, which is comprised of a polarizer, a switchable 90° TN cell and a quarter-wave ($\lambda/4$) plate, is used to convert the incident light into circularly polarized light and switch its handedness. When the TN cell is at voltage-off state, it serves as a broadband polarization rotator [20,21], rotating the input linear polarization by 90° . When applying voltage on the TN cell, the polarization rotator is switched off, leaving the input polarization unaltered. Hence, in combination with the $\lambda/4$ plate, the handedness of the circular polarization can be switched by the TN cell. Two CLC films have opposite handedness. For a CLC film, circularly polarized light would be $\sim 100\%$ reflected if its handedness coincides with the helical chirality of the CLC and its wavelength within the reflection band; while the opposite circular polarization would be simply transmitted.

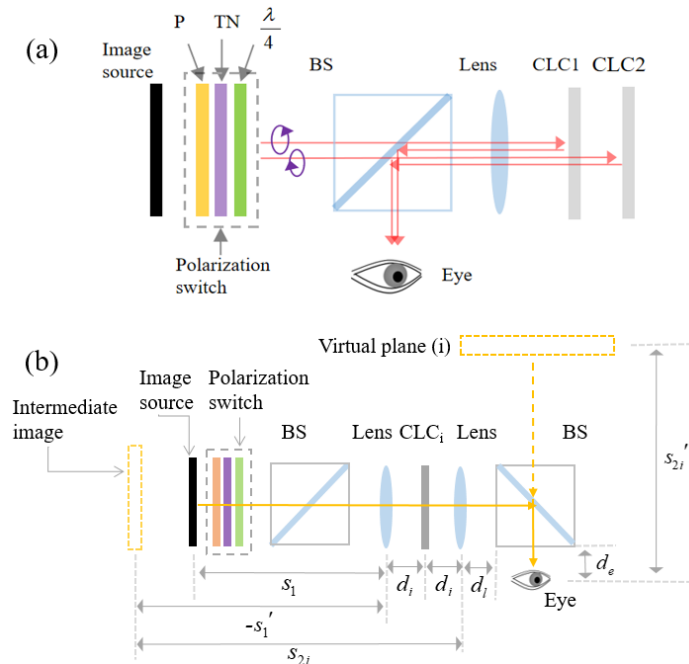


Fig. 1. (a) System design of a proposed multi-plane display with two CLC films. The optical paths of LH and RH circularly polarized light are denoted by anticlockwise and clockwise arrows, respectively. P is polarizer, CLC1 is RH and CLC2 is LH. $\lambda/4$ is quarter-wave plate. (b) Unfolded optical path of RH or LH circular polarization.

Let's assume the polarizer and $\lambda/4$ plate have been adjusted to convert the incident light into left-handed (LH) circularly polarized light when the TN cell is applied with voltage. The

CLC1 film has right-handed (RH) chirality, while the CLC2 film is LH. At one moment, with the TN cell on, the generated LH circularly polarized light (anticlockwise arrow), is reflected by the CLC2 film. At the next moment when the voltage is removed, the image light becomes RH circularly polarized, and is then reflected by the CLC1 film. Due to the different positions of the two CLC films, LH and RH light undergoes different optical path length, and thus is imaged at different depths by the lens, after passing through it twice. By switching the TN cell in accordance with the image source rapidly, a flicker-free dual-plane 3D AR display could be realized in time sequence.

The virtual image depths can be calculated using the Gaussian form of the lens equation. Assume the distance from the image source to the lens is s_1 , the focal length of the lens is f , and the distance from the lens to CLC1 and CLC2 are d_1 and d_2 , respectively. Because $s_1 < f$, as light from the image source passes through the lens for the first time, a magnified-virtual-intermediate image is generated in front of the lens. The distance from the lens to the intermediate image s_1' should satisfy:

$$\frac{1}{f} = \frac{1}{s_1} + \frac{1}{s_1'}. \quad (1)$$

If the intermediate image is in front of the lens, s_1' is negative; and if it is behind the lens, s_1' is positive. When the light from the intermediate image is reflected by one of the CLC films, and encounters the lens for the second time, the effective distance from the intermediate image to the lens s_{2i} is:

$$s_{2i} = 2d_i - s_1', \quad (2)$$

where $i=1,2$ for the light reflected by CLC1 and CLC2, respectively.

So after light passes through the lens for the second time, a final image is generated. The distance from the lens to the final image s_{2i}' should satisfy:

$$\frac{1}{f} = \frac{1}{s_{2i}} + \frac{1}{s_{2i}'}. \quad (3)$$

From Eqs. (1) (2) and (3), we can obtain s_{2i}' if d_i is equal to d_e :

$$s_{2i}' = \frac{2d_i f (s_1 - f) - s_1 f^2}{2d_i (s_1 - f) - (2s_1 - f) f}. \quad (4)$$

For example, when $s_1 = 43$ mm, $f = 103$ mm, $d_1 = 4$ mm, and $d_2 = 13$ mm, we can obtain $s_{21}' = -400$ mm and $s_{22}' = -3.2$ m. The negative sign indicates the final image is located in front of the lens. When the BS and lens are placed closely, with the configuration in Fig. 1, the two virtual images are displayed approximately at 400 mm and 3.2 m in front of the outer surface of the BS, respectively.

3. Experiment and results

In our experiment, we prepared two CLC materials with opposite handedness, using the same nematic liquid crystal (Changchun Institute of Optics, Fine Mechanics and Physics, Chinese Academy of Science) with large birefringence $\Delta n \sim 0.4$. The chiral dopant used in the RHCLC sample was R5011 (HCCH, China), and its weight percentage was $\sim 2.95\%$; In the LHCLC,

3% S5011 (HCC, China) was doped. Then we infiltrated the LC mixtures into 10 μm homogeneous cells. In order to avoid surface reflection, anti-reflection glass pieces (refractive index $n \sim 1.46$) were attached to both sides of each cell, and the gaps were filled with an index-matching liquid, glycerol (refractive index $n \sim 1.47$). Uniform cholesteric phase was formed after the application of a short electric field pulse, and the pictures of the fabricated films (attached with anti-reflection glasses) are shown as the insets of Fig. 2.

To determine the reflection band of the CLC films, we measured their transmittance spectra using a high resolution spectrometer (Ocean Optics). The bandwidth of both CLC films are ~ 120 nm as shown in Fig. 2. The RHCLC band is from 513 nm to 630 nm, and the LHCLC band is from 523 nm to 644 nm. The broad overlapped band (>100 nm), enables the implementation of color display using the CLC films. Employing pitch gradient or multi-layer technique [23], we could expand the reflection band of the CLC films and thus realize full-color display.

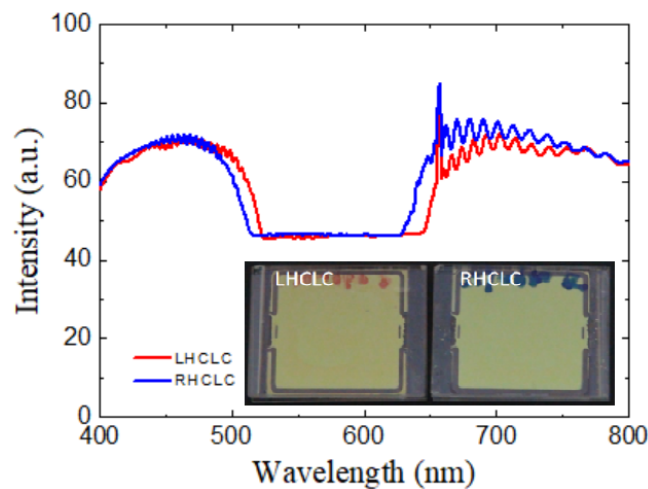


Fig. 2. Reflection band of the LHCHC (red curve) and RHCLC (blue curve). Insets show the fabricated CLC films attached with anti-reflection glass pieces.

To quantitatively investigate their reflective properties, we measured the reflectance of the CLC films using circularly polarized laser light at two wavelengths: 532 nm and 633 nm. The measured results are shown in Table 1. One can see that for both films, the contrast ratio (CR), between the reflections of polarization matched light and mismatched light, is reasonably high. Now the laser wavelengths, 532 nm and 633 nm, are near the edge of the reflection band of the CLC films, so if the reflection band is expanded, the contrast ratio of green and red colors could be further improved. The CR of the LHCLC film was slightly better than that of the RHCLC. This could be attributed to the fact that 633 nm is nearer the edge of the reflection band for the RHCLC film.

Table 1. Reflectance of the fabricated CLC films for circular polarizations.

| Laser | Circular polarization | Reflectance (LHCLC) | Reflectance (RHCLC) |
|--------|-----------------------|---------------------|---------------------|
| 532 nm | Left-handed | 99.3% | 2.86% |
| | Right-handed | 2.8% | 97.2% |
| 633 nm | Left-handed | 96.6% | 3.9% |
| | Right-handed | 3.7% | 95.5% |

To verify the feasibility of the proposed scheme in Fig. 1, we implemented a mono-color dual plane AR display system using off-the-shelf optical components and a green laser (532 nm). Due to the lack of appropriate focal-length lens, we used two lenses and two BSs in the system, to mimic the unfolded optical path in Fig. 1. Lens L1 ($f_1 = 100$ mm) was placed between the polarization switch and CLC films to generate an intermediate image of the image source with the same size. The original lens before CLC films was removed. Lens L2 ($f_2 = 60$ mm) was placed immediately after the CLC films, and a second BS was set before the eye. Comparing this setup with the unfolded light path in Fig. 1(b), we could see that they are almost equivalent if the focal length of L1 was equal to L2.

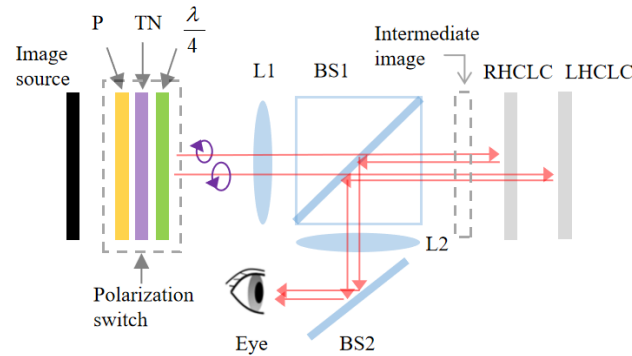


Fig. 3. Experimental setup of the dual-plane AR system.

If both the TN cell and image source can be switched rapidly, the LH and RH circularly polarized images would be observed simultaneously because of the persistence of human eye; and a flicker-free dual-plane AR display could be realized. To achieve fast response time, a 3 μm TN cell was filled with a low viscosity liquid crystal HSG09400-100 (HCCH, China, $\Delta n = 0.156$ and $\Delta\epsilon = 2.4$). Its rise time and decay time were 3.52 ms and 520 μs , respectively. In the experiment, the system was operated at a frequency of 50 Hz, indicating a frame rate of 25 Hz for the dual-plane 3D display. This frame rate is sufficient for video-rate 3D image reconstruction. According to Wu et al., by using a higher birefringence LC material with a thinner cell gap, submillisecond response could be obtained for the TN cell [15], and thus higher frame rate could be realized.

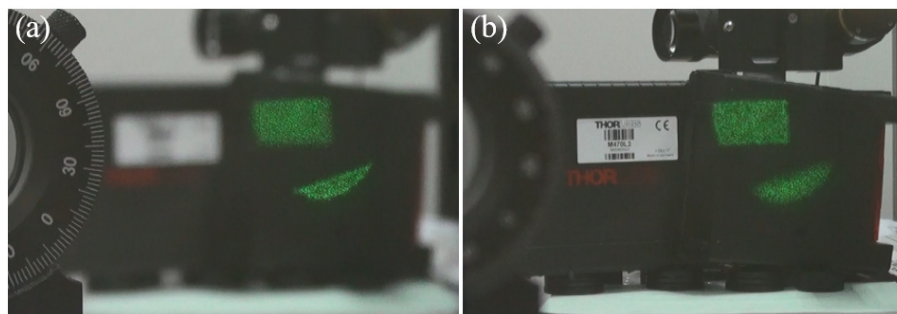


Fig. 4. Displayed images by the dual-plane AR display system when the camera was focused at (a) 20 cm and (b) 130 cm, respectively.

In our experiment, we used a diffusive screen with laser projection as the image source because it could be conveniently synchronized with the TN cell. The image source is synchronized with the TN cell. At one moment, when a “moon” shaped image was displayed on the screen, the TN cell was turned off, generating RH circular polarization. At the next moment, a “rectangle” shaped image was displayed, and the TN cell was turned on,

generating LH circular polarization. So the “moon” and the “rectangle” were reflected by the RHCLC and LHCLC, and imaged at two different depths, 20 cm and 130 cm, respectively. The captured images through BS2 are shown in Fig. 4. There were two real objects (part of a polarizer and a label on a box) placed at 20 cm and 130 cm, respectively, for comparison. When the camera was focused at 20 cm, as shown in Fig. 4(a), both the “moon” and the polarizer were clearly observed, while the “rectangle” was blurred. When the camera was focused at 130 cm, as shown in Fig. 4(b), both the “rectangle” and the label were clearly observed, while the “moon” and polarizer were blurred. Therefore, the system provided the focus cues correctly, and thus could effectively solve the accommodation-convergence conflict.

We also implemented a color AR display using a mobile phone as its image source. Figures 5(a) and 5(b) are photos captured through BS2, when the incident light impinged on the CLC films with RH circular polarization. A virtual image, “flower” was imaged at 20 cm away from the camera. Figures 5(c) and 5(d) are photos captured when the incident light upon the CLC films was LH circularly polarized. The “flower” was then imaged at a farther position, 130 cm from the camera. Because of correct accommodation depth cue presented in the system, one can always see the blurring effect for out-of-focus objects, no matter they are real or virtual. In this color-display experiment, the optical switch in Fig. 3 was replaced by broadband circular polarizers (400-700 nm, Edmund Optics) for the sake of better extinction ratio for both red and green colors.

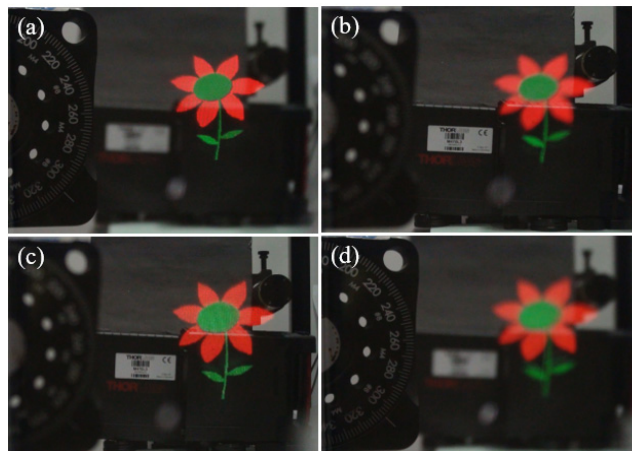


Fig. 5. RH circularly-polarized virtual “flower” imaged at 20 cm: camera focused at (a) 20 cm and (b) 130 cm, respectively. LH circularly-polarized virtual “flower” imaged at 130 cm: camera focused at (c) 130 cm and (d) 20 cm, respectively.

Besides, we investigated the ability of displaying an overlapping color using our system experimentally. Figure 6 shows a yellow left-handed star displayed at 1 m, and a reference object, a label placed at 1 m. Apparently, our system is capable of displaying overlapping color.



Fig. 6. A yellow star imaged at 1 m away, and the camera was focused at 1m.

In addition, we measured the field of view and eye box size of our system, which were $\sim 23^\circ$ diagonally and 12 mm, respectively. The monocular images have some granularity, which is caused by the texture of diffusive screen. By using a LCD as the display source, one can see that generated color images in Fig. 5 have much better image quality.

To extend the above scheme for multi-plane displays to provide more than 2 image planes, we proposed the system design as plotted in Fig. 7. Here, switchable $\lambda/2$ plates and CLC films, are placed alternatively in space so that light from the image source can be selectively reflected by one of the CLC films by controlling the on-and-off states of $\lambda/2$ plates. For example, assuming the image light is LH circularly polarized (by appropriate arranging of the polarizer and $\lambda/4$ plate), and all the CLC films have right handedness, light would be reflected by the k^{th} CLC film if the k^{th} $\lambda/2$ is turned on while all the other $\lambda/2$ plates are turned off. By selecting the 1st, 2nd, ..., N^{th} $\lambda/2$ plate rapidly in time sequence, light would be reflected by a CLC film one by one, and virtual images would be generated at different depths by the lens. Hence, a multi-plane AR display could be realized. In general cases, it is not necessary to make all the CLC films with the same helical handedness, as long as the $\lambda/2$ plates can be individually controlled. The switchable $\lambda/2$ plates, which are usually made of thin liquid crystal cells [22], can be stacked closely with the CLC films. Thus a compact form factor can be realized for this multi-plane AR display.

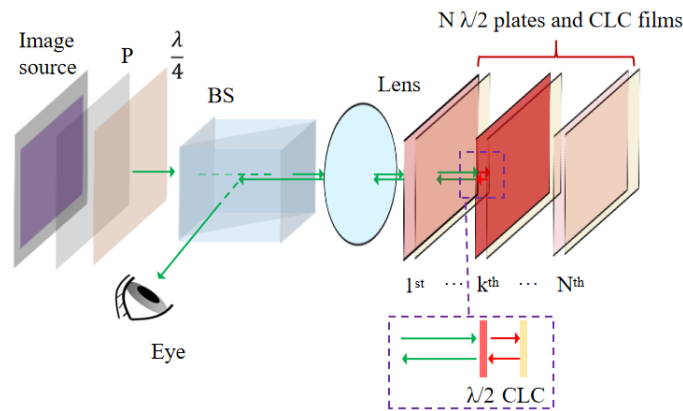


Fig. 7. Multi-plane AR display design by stacking switchable $\lambda/2$ plates and CLC films. Green arrows—RH circularly polarized light, and red arrows—LH circularly polarized light.

We carried out a proof-of-concept experiment using three RHCLC films and a LH circularly polarized image source. When a half wave plate was inserted in front of the first, second and third RHCLC film, the final virtual image was displayed at 20 cm, 50 cm, and 110 cm, respectively. As shown in Fig. 8, in the 110 cm case, when the camera was focused on

the virtual image (110 cm), both the image and a real object (a Thorlabs label also at 110 cm) were clear in focus; when the camera was focused at 50 cm, both the virtual image and Thorlabs label are blurred. Hence, the feasibility of this scheme is verified.

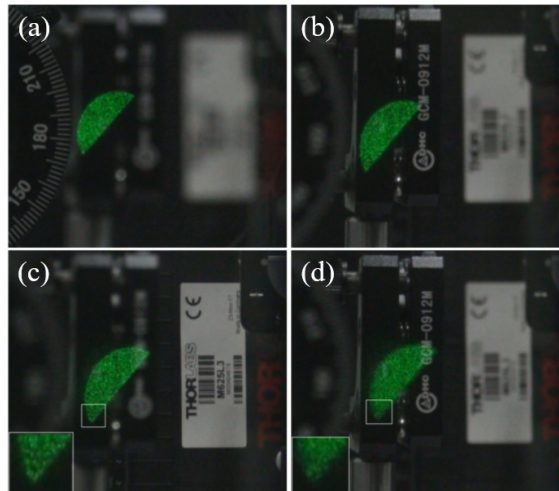


Fig. 8. Images displayed at (a) 20 cm (b) 50 cm (c) 110 cm (d) 110 cm when the camera was focused at (a) 20 cm (b) 50 cm (c) 110 cm (d) 50 cm, respectively.

4. Discussion

In the experiment, CLC cells with ITO glass substrates were used instead of standalone CLC films. To achieve a smaller form factor and lighter weight, one can employ CLC polymer films using the fabrication method reported in Ref [24]. In our system, the optical efficiency varies as different types of light sources are used. For light sources with linearly polarized light such as a LCD, maximum optical efficiency could be achieved by appropriately orientating the polarizer in the polarization switch. If circularly polarized or unpolarized light is used, however, there would be considerable amount of light loss due to the absorption of the polarizer.

5. Conclusion

In this paper, we proposed a compact multi-plane AR display system employing a polarization switch and CLC films. Because of the polarization selectivity of CLC films, LH and RH circular polarizations undergo different optical path lengths through the lens, forming virtual images at different depths. A proof-of concept monocular dual-plane AR display system was demonstrated, and its color display capability was verified. With low driving voltage and simple implementation, the proposed system could render all depth cues correctly and thus solves the accommodation-convergence conflict problem. Moreover, it could be easily extended to a multi-plane AR display with more than 2 planes, by stacking multiple polarization switches and CLC films together, without much sacrifice of its form factor. The proposed scheme could be attractive for various applications such as near eye displays, augmented reality and 3D displays.

Funding

National Natural Science Foundation of China (61727808); Shanghai Jiao Tong University (YG2016QN37); Key Lab of Advanced Optical Manufacturing Technologies of Jiangsu Province & Key Lab of Modern Optical Technologies of Education Ministry of China, Soochow University (KJS1607).

References

1. J. Geng, "Three-dimensional display technologies," *Adv. Opt. Photonics* **5**(4), 456–535 (2013).
2. D. M. Hoffman, A. R. Girshick, K. Akeley, and M. S. Banks, "Vergence-accommodation conflicts hinder visual performance and cause visual fatigue," *J. Vis.* **8**(3), 33 (2008).
3. G. Li, D. Lee, Y. Jeong, J. Cho, and B. Lee, "Holographic display for see-through augmented reality using mirror-lens holographic optical element," *Opt. Lett.* **41**(11), 2486–2489 (2016).
4. P. Zhou, Y. Li, S. Liu, S. Huang, Q. Chen, and Y. Su, "Holographic see-through AR display with zero-order eliminated," *SID Symp. Digest* **48**(1), 1638–1640 (2017).
5. H. Hua and B. Javidi, "A 3D integral imaging optical see-through head-mounted display," *Opt. Express* **22**(11), 13484–13491 (2014).
6. M.-Y. He, H.-L. Zhang, H. Deng, X.-W. Li, D.-H. Li, and Q.-H. Wang, "Dual-view-zone tabletop 3D display system based on integral imaging," *Appl. Opt.* **57**(4), 952–958 (2018).
7. Y. Takaki, Y. Urano, S. Kashiwada, H. Ando, and K. Nakamura, "Super multi-view windshield display for long-distance image information presentation," *Opt. Express* **19**(2), 704–716 (2011).
8. S.-K. Kim, E.-H. Kim, and D.-W. Kim, "Full parallax multifocus three-dimensional display using a slanted light source array," *Opt. Eng.* **50**(11), 114001 (2011).
9. X. Hu and H. Hua, "Design and assessment of a depth-fused multi-focal-plane display prototype," *J. Disp. Technol.* **10**(4), 308–316 (2014).
10. H.-S. Chen, Y.-J. Wang, P.-J. Chen, and Y.-H. Lin, "Electrically adjustable location of a projected image in augmented reality via a liquid-crystal lens," *Opt. Express* **23**(22), 28154–28162 (2015).
11. S. Liu, Y. Li, P. Zhou, X. Li, N. Rong, S. Huang, W. Lu, and Y. Su, "A multi-plane optical see-through head mounted display design for augmented reality applications," *J. Soc. Inf. Disp.* **24**(4), 246–251 (2016).
12. S. Liu, Y. Li, P. Zhou, Q. Chen, and Y. Su, "Reverse-mode PSLC multi-plane optical see-through display for AR applications," *Opt. Express* **26**(3), 3394–3403 (2018).
13. Y.-H. Lee, H.-W. Chen, R. Martinez, Y. Sun, S. Pang, and S.-T. Wu, "Multi-image plane display based on polymer-stabilized cholesteric texture," *SID Symp. Digest* **48**(1), 760–762, (2017).
14. G. D. Love, D. M. Hoffman, P. J. W. Hands, J. Gao, A. K. Kirby, and M. S. Banks, "High-speed switchable lens enables the development of a volumetric stereoscopic display," *Opt. Express* **17**(18), 15716–15725 (2009).
15. Y.-H. Lee, F. Peng, and S.-T. Wu, "Fast-response switchable lens for 3D and wearable displays," *Opt. Express* **24**(2), 1668–1675 (2016).
16. C.-K. Lee, S. Moon, S. Lee, D. Yoo, J.-Y. Hong, and B. Lee, "Compact three-dimensional head-mounted display system with Savart plate," *Opt. Express* **24**(17), 19531–19544 (2016).
17. S.-T. Wu and D.-K. Yang, *Reflective Liquid Crystal Displays* (Wiley, 2001).
18. M. Mitov and N. Dessaud, "Going beyond the reflectance limit of cholesteric liquid crystals," *Nat. Mater.* **5**(5), 361–364 (2006).
19. D.-K. Yang and S.-T. Wu, *Fundamentals of Liquid Crystal Devices* (Wiley, 2006).
20. M. Schadt and W. Helfrich, "Voltage-dependent optical activity of a twisted nematic liquid crystal," *Appl. Phys. Lett.* **18**(4), 127–128 (1971).
21. C. H. Gooch and H. A. Tarry, "The optical properties of twisted nematic liquid crystal structures with twist angles $\leq 90^\circ$," *J. Phys. D: Appl. Phys.* **8**(13), 1575–1584 (1975).
22. M. D. Lavrentovich, T. A. Sergan, and J. R. Kelly, "Switchable broadband achromatic half-wave plate with nematic liquid crystals," *Opt. Lett.* **29**(12), 1411–1413 (2004).
23. M. Mitov, "Cholesteric liquid crystals with a broad light reflection band," *Adv. Mater.* **24**(47), 6260–6276 (2012).
24. Y. Zhou, E. E. Jang, Y. Huang, and S.-T. Wu, "Enhanced laser emission in opposite handedness using a cholesteric polymer film stack," *Opt. Express* **15**(6), 3470–3477 (2007).